Differentiating Electromechanical From Non–Electrical Substrates of Mechanical Discoordination to Identify Responders to Cardiac Resynchronization Therapy

Joost Lumens, PhD; Bhupendar Tayal, MD; John Walmsley, PhD; Antonia Delgado-Montero, MD; Peter R. Huntjens, MSc; David Schwartzman, MD; Andrew D. Althouse, PhD; Tammo Delhaas, MD, PhD; Frits W. Prinzen, PhD; John Gorcsan III, MD

Background—Left ventricular (LV) mechanical discoordination, often referred to as dyssynchrony, is often observed in patients with heart failure regardless of QRS duration. We hypothesized that different myocardial substrates for LV mechanical discoordination exist from (1) electromechanical activation delay, (2) regional differences in contractility, or (3) regional scar and that we could differentiate electromechanical substrates responsive to cardiac resynchronization therapy (CRT) from unresponsive non–electrical substrates.

Methods and Results—First, we used computer simulations to characterize mechanical discoordination patterns arising from electromechanical and non–electrical substrates and accordingly devise the novel systolic stretch index (SSI), as the sum of posterolateral systolic prestretch and septal systolic rebound stretch. Second, 191 patients with heart failure (QRS duration ≥120 ms; LV ejection fraction ≤35%) had baseline SSI quantified by automated echocardiographic radial strain analysis. Patients with SSI≥9.7% had significantly less heart failure hospitalizations or deaths 2 years after CRT (hazard ratio, 0.32; 95% confidence interval, 0.19–0.53; $P<0.001$) and less deaths, transplants, or LV assist devices (hazard ratio, 0.28; 95% confidence interval, 0.15–0.55; $P<0.001$). Furthermore, in a subgroup of 113 patients with intermediate electrocardiographic criteria (QRS duration of 120–149 ms or non–left bundle branch block), SSI≥9.7% was independently associated with significantly less heart failure hospitalizations or deaths (hazard ratio, 0.41; 95% confidence interval, 0.23–0.79; $P=0.004$) and less deaths, transplants, or LV assist devices (hazard ratio, 0.27; 95% confidence interval, 0.12–0.60; $P=0.001$).

Conclusions—Computer simulations differentiated patterns of LV mechanical discoordination caused by electromechanical substrates responsive to CRT from those related to regional hypocontractility or scar unresponsive to CRT. The novel SSI identified patients who benefited more favorably from CRT, including those with intermediate electrocardiographic criteria, where CRT response is less certain by ECG alone. **(*Circ Cardiovasc Imaging*. 2015;8:e003744. DOI: 10.1161/CIRCIMAGING.115.003744.)**

Key Words: bundle branch block ■ CircAdapt ■ dyssynchrony ■ echocardiography ■ heart failure ■ myocardial scar ■ strain

Current clinical guidelines for cardiac resynchronization therapy (CRT) in heart failure (HF) patients with low left ventricular ejection fraction (LVEF) are based on electrocardiographic criteria, including QRS prolongation and morphology.[1] Lack of response to CRT remains an important clinical problem. Although HF patients with regional LV mechanical discoordination, often called mechanical dyssynchrony when derived from time-to-peak regional LV strain measurements, have been shown to respond more favorably to CRT,[2,3] the routine use of mechanical discoordination as an adjunct to the electrocardiographic criteria for patient selection for CRT has not gained clinical acceptance.[1,4] Furthermore, CRT has been shown to have no beneficial effect or even harm patients with LV mechanical dyssynchrony and narrow QRS duration.[5,6] The strongest evidence for positive response to CRT is in patients with left bundle branch block (LBBB) and QRS duration ≥150 ms,[7] whereas all of the large randomized clinical trials investigating the effects of CRT also included patients with non-LBBB morphology and QRS duration ≥120[8] or ≥130 ms.[9,10] The result is clinical uncertainty for benefit of CRT in patients with intermediate electrocardiographic criteria, specifically those with QRS duration of 120 to 149 ms or non-LBBB morphology.[1] Accordingly, there is a clinical need to enhance mechanistic understanding of LV mechanical discoordination which may potentially improve patient selection in those with intermediate electrocardiographic criteria.

See Editorial by Delgado and Bax
See Clinical Perspective

Received March 9, 2015; accepted August 7, 2015.

From the CARIM School for Cardiovascular Diseases, Maastricht University Medical Center, Maastricht, The Netherlands (J.L., J.W., P.R.H., T.D., F.W.P.); L'Institut de Rythmologie et Modélisation Cardiaque (IHU-LIRYC), Pessac-Bordeaux, France (J.L., P.R.H.); and Heart and Vascular Institute, University of Pittsburgh Medical Center, PA (B.T., A.D.-M., D.S., A.D.A., J.G.).

The Data Supplement is available at http://circimaging.ahajournals.org/lookup/suppl/doi:10.1161/CIRCIMAGING.115.003744/-/DC1.

Correspondence to Joost Lumens, PhD, CARIM School for Cardiovascular Diseases, Maastricht University Medical Center, PO Box 616, 6200 MD Maastricht, The Netherlands. E-mail joost.lumens@maastrichtuniversity.nl

We hypothesized that the origin of mechanical discoordination is diverse and that it may arise not only from electromechanical substrates responsive to CRT but also from non–electrical substrates, such as regional myocardial scar or hypocontractility, that are unresponsive to CRT. We further hypothesized that we could identify the electromechanical substrate responsive to CRT using myocardial strain characteristics. We tested these hypotheses in a 2-part study. First, computer simulations were used to characterize patterns of LV mechanical discoordination arising from (1) electrical activation delay, (2) regional differences in contractility, and (3) regional myocardial scar, alone or in combination. Based on these simulations, we devised a novel systolic stretch index (SSI), defined as the sum of posterolateral systolic prestretch (SPS_{POST}) and septal systolic rebound stretch (SRS_{SEPT}), which characterized the electromechanical substrate responsive to CRT. Second, we studied a consecutive clinical series of HF patients with routine indications for CRT to determine associations of SSI with the predefined clinical outcome variables of HF hospitalizations, death, heart transplant, or LV assist device (LVAD) implantation. Finally, we performed a subgroup analysis to assess the association of SSI with outcome after CRT in patients with intermediate electrocardiographic criteria for whom clinical benefit of CRT is uncertain.

Methods

Computer Simulations

The CircAdapt computational model of the human heart and circulation[11] (www.circadapt.org) was used to simulate local ventricular myofiber mechanics in hearts with different degrees and combinations of electromechanical and non–electrical substrates of mechanical discoordination. CircAdapt has previously been shown to realistically simulate cardiovascular system mechanics and hemodynamics in the dyssynchronous failing heart treated with CRT.[12–15]

Reference HF Simulation

Starting from a simulation representing the normal adult heart, diffuse myocardial hypokinesis was induced by a global 50% reduction of myofiber contractility, and dilation of all wall segments until LVEF was 28%. Heart rate and cardiac output were set to mean values measured in the patient cohort, that is, 71 bpm and 3.2 L/min, respectively. Circulating blood volume and peripheral vascular resistance of the systemic circulation were adjusted so that mean arterial pressure equaled 92 mm Hg. Ventricular walls were subdivided into segments (Figure 1A, left panel) comparable with the standard midventricular short-axis segmentation used during echocardiographic strain imaging. All ventricular segments were synchronously activated 200 ms after right atrial activation, representing prolonged atrioventricular conduction.[15]

Simulations of Electromechanical and Non–Electrical Substrates

Starting from the reference HF simulation, 3 different substrates of contraction heterogeneity were simulated:

1. Electromechanical substrate: LBBB-like ventricular activation patterns with maximal posterior activation delays of 50, 100, and 150 ms (Figure 1A).
2. Non–electrical hypocontractility substrate: 3 degrees of posterolateral contractility decrease, mimicking reduced ability of the myocardium to generate active tension (Figure 1B).[16]
3. Non–electrical scar substrate: 3 degrees of posterolateral scar were simulated in the hypocontractility simulations by additionally increasing passive stiffness, mimicking fibrotic myocardial remodeling (Figure 1C).[16]

We performed 28 different HF simulations based on all possible combinations of the electromechanical and non–electrical substrates above.

Differentiating Electromechanical From Non–Electrical Substrates

The simulations were used to identify the radial strain characteristics specific for different substrates of LV mechanical discoordination. This mechanistic knowledge was used to design a radial strain–based index sensitive to the electromechanical substrates responsive to CRT and relatively insensitive to non–electrical substrates. This novel index, called SSI, is calculated in 5 steps:

1. Calculate mean LV radial strain (Figure 2A).
2. Subtract the mean LV radial strain pattern from all local strain patterns, resulting in mean-centered strain patterns (Figure 2B), that is, the local deviation from mean radial deformation; mean centering was applied to minimize the effect of global deformation artifacts.
3. Average the mean-centered strain patterns of the 2 septal and the 2 posterolateral segments (Figure 2C).
4. Calculate SPS_{POST} (Figure 2C), as stretch occurring between time of onset QRS and aortic valve opening (AVO); calculate SRS_{SEPT} (Figure 2C), defined as stretch following initial shortening between time of onset QRS and aortic valve closure.[17]
5. Calculate SSI by summing SRS_{SEPT} and SPS_{POST}.

Custom-made software (Matlab 7.11.0, MathWorks, Natick, MA) was developed for automatic SSI calculation using 6 regional time–strain curves and time of onset QRS, AVO, and aortic valve closure as input. Comparisons were also made with the clinical indices of interventricular mechanical delay (IVMD), defined as the time difference between pulmonary and aortic valve opening, and peak-to-peak radial strain delay, defined as the time between earliest septal or anteroseptal peak strain and latest posterior or lateral peak strain.[18]

Simulations of Acute Response to CRT

For all baseline HF simulations, CRT was simulated by acutely imposing a ventricular activation pattern mimicking simultaneous biventricular pacing at a paced atrioventricular delay of 120 ms. During CRT, activation spreads with an intersegment delay of 40 ms (Figure I in the Data Supplement), resulting in a total ventricular activation time of 80 ms. Acute hemodynamic response to CRT was defined as the percentage change of LV stroke volume.

Clinical Study

The study design was prospective with novel analysis applied to an existing patient database by investigators blinded to all clinical data and predefined clinical end points. The protocol for the patient study was approved by the Institutional Review Board for Biomedical Research of University of Pittsburgh Medical Center. All patients gave informed consent consistent with this protocol.

Patients

The study group began with 210 consecutive New York Heart Association Class II to IV HF patients with QRS duration ≥120 ms and LVEF ≤35% referred for CRT with routine indications. Nineteen patients (9%) were prospectively excluded because echocardiographic images were unsuitable for quantitative strain analysis. Table 1 shows baseline characteristics for the resulting cohort of 191 patients. No patients had atrial fibrillation. All patients were on optimal pharmacological therapy. CRT was initiated after routine biventricular pacing system implantation with LV lead placement in epicardial veins targeting the posterior or lateral wall. No leads were placed in anteroseptal or inferoseptal regions.

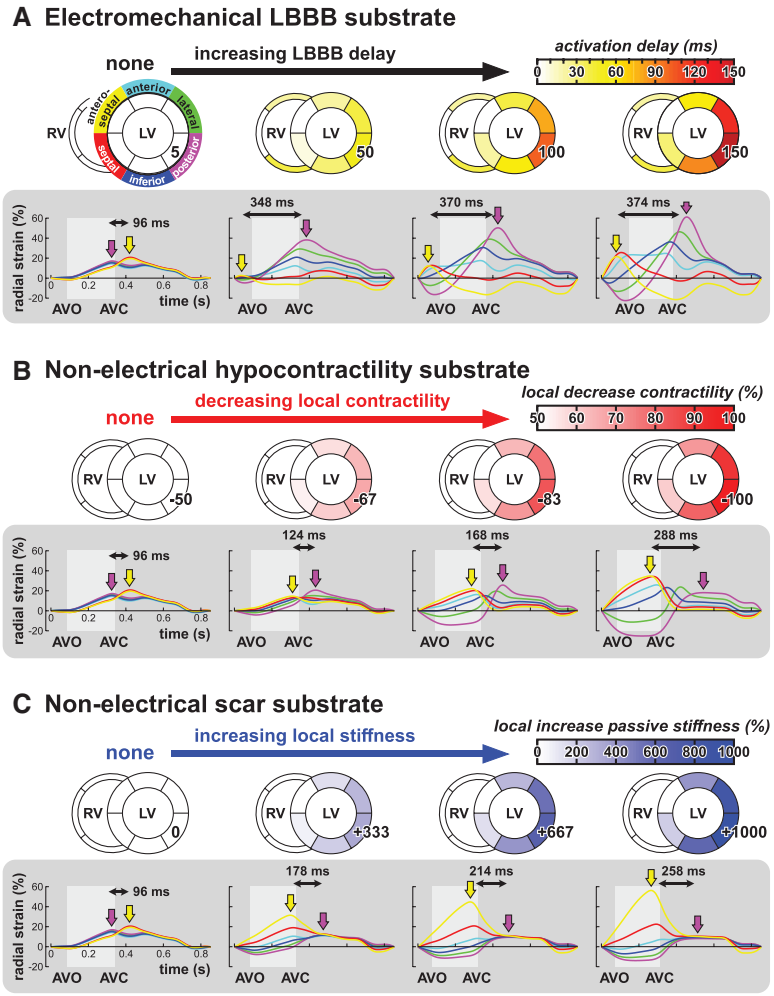

Figure 1. Simulated substrates of mechanical discoordination. **A**, An electromechanical left bundle branch block (LBBB) substrate simulated as a septal-to-free wall gradient in activation delay. **B**, A non–electrical hypocontractility substrate simulated as a septal-to-free wall gradient in contractility. **C**, A non–electrical scar substrate simulated by adding a septal-to-free wall gradient in passive stiffness to the hypocontractility substrate is shown in **B**. All 3 substrates caused peak-to-peak radial strain delay but the pattern of mechanical discoordination differs considerably between the substrates. Peak septal (yellow arrow) and posterior (purple arrow) radial strains were used to quantify peak-to-peak radial strain delay (black double-headed arrows). AVC indicates aortic valve closure; AVO, aortic valve opening; LV, left ventricle; and RV, right ventricle.

Baseline Echocardiography

The following echocardiographic protocol was performed before CRT device implantation. Routine apical 4-chamber and 2-chamber views were used for quantification of LV volumes and LVEF using biplane Simpson's rule. Times of AVO and closure were determined from routine pulsed wave Doppler spectral recordings. Radial strain was acquired from the mid LV short-axis view as previously described.[18] Strain analysis was performed on a minimum of 3 beats and did not require a fixed beat-to-beat interval; no patients were in atrial fibrillation. Briefly, endocardial and epicardial borders were manually traced to create a region of interest, which was adjusted to accomplish optimal tracking (GE EchoPac BT11, Horten, Norway). The 6 LV regional time–strain curves were exported to a remote laboratory (Maastricht University) where fully automated SSI analysis was performed, using custom-made software, by investigators who were blinded to all clinical outcome data. Interobserver and intraobserver

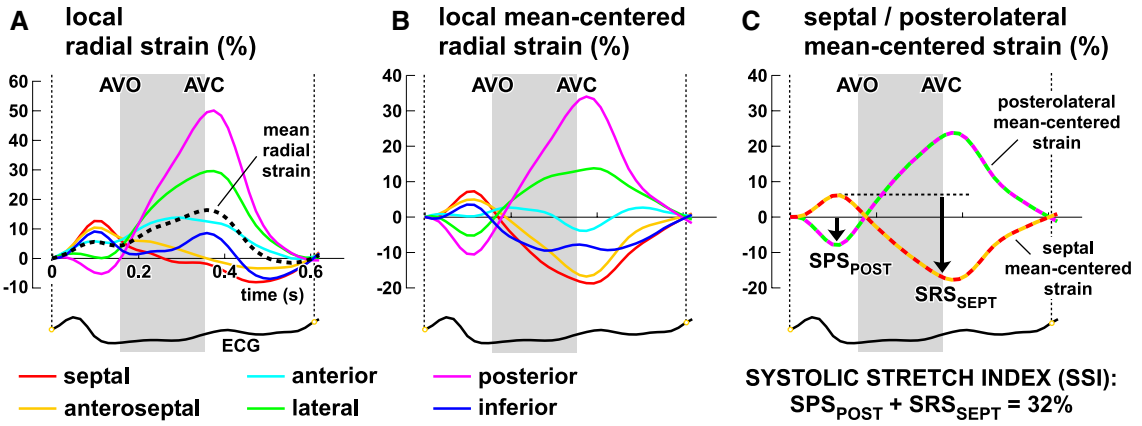

Figure 2. Calculation of the systolic stretch index (SSI). Radial strain data from a patient with QRS duration of 168 ms and left bundle branch block. Vertical dotted lines indicate onset QRS. SSI is obtained by (**A**) calculating mean left ventricular (LV) radial strain (dashed line); (**B**) mean-centering regional radial strains, by subtracting the mean LV radial strain pattern from all regional strain patterns; (**C**) calculating and summing posterolateral systolic prestretch (SPS_{POST}) and septal systolic rebound stretch (SRS_{SEPT}).

Table 1. Baseline Characteristics of the Overall Sample Grouped by Baseline SSI

Variables	Total Sample, n=191	SSI≥9.7%, n=103	SSI<9.7%, n=88	*P* Value
Age, y	66±11	64±11	68±11	0.04*
Sex, male	141 (74%)	67 (65%)	74 (84%)	0.003*
Ischemic disease, n	115 (60%)	52 (51%)	63 (72%)	0.003*
Diabetes mellitus, n	61 (32%)	29 (28%)	32 (36%)	0.64
NYHA II/III, n	145 (76%)	79 (83%)	66 (80%)	0.70
LBBB, n	115 (60%)	71 (69%)	44 (50%)	0.01*
QRS duration, ms	159±27	163±26	154±27	0.02*
β-blocker, n	165 (87%)	90 (88%)	77 (86%)	0.83
ACE/ARB inhibitor, n	165 (87%)	89 (87%)	76 (87%)	1.00
LVEF	24±6	25±6	24±7	0.26

ACE indicates angiotensin-converting enzyme; ARB, angiotensin II receptor blocker; LBBB, left bundle branch block; LVEF, left ventricular ejection fraction; NYHA, New York Heart Association; and SSI, systolic stretch index.

*P<0.05 SSI≥9.7% vs SSI<9.7%.

variability analyses of computerized SSI calculations were performed by repeated speckle-tracking radial strain analysis (including tracing of endocardial and epicardial borders and SSI calculation) in a random sample of 20 patients by 2 different investigators. The intraclass correlation coefficient for SSI as a continuous variable was 0.94 for interobserver agreement, indicating good reproducibility across different reviewers, and 0.92 for intraobserver agreement, indicating good reproducibility within the same reviewer. When evaluating agreement for SSI<9.7%, there was 90% interobserver agreement (κ=0.8) and 90% intraobserver agreement (κ=0.8).

Clinical Follow-Up and Predefined Subgroup Analysis

Patients were followed clinically for a 2-year period, with predefined combined end points. The primary end point was time to HF hospitalization or death, whichever came first. The combined secondary end point was death, heart transplant, or LVAD therapy. The rescue therapies of transplant or LVAD were combined as end points with death because only patients with a limited life expectancy receive these treatments at our institution. Echocardiographic follow-up data on LV volumes at 6 months after CRT were available for 155 patients (81%). These data were used to determine the cutoff value of SSI using a predefined independent definition of CRT response as a decrease in LV end-systolic volume ≥15%. A predefined subgroup of patients was identified with intermediate electrocardiographic criteria, where clinical usefulness of CRT is less clearly defined (currently by guideline class IIa or IIb indications), namely those with QRS duration of 120 to 149 ms or non-LBBB electrocardiographic morphology.[1]

Statistical Analysis

Reproducibility of the SSI was assessed using intraclass correlation coefficients. Pearson's correlation coefficient was used to assess the correlation between mechanical discoordination indices (peak-to-peak radial strain delay, SSI) and acute changes in LV stroke volume. Receiver operator characteristic curve analysis was used to determine an SSI cutoff (with CRT response defined as a LV end-systolic volume decrease of ≥15% at 6 months and no unfavorable event). Patients were divided into groups (SSI<9.7% versus SSI≥9.7%); all group data were presented as mean±SD (continuous variables) or frequencies and percentages (categorical variables). Continuous variables are compared between groups using Student *t* test, and categorical variables are compared using Fisher's exact test. Freedom from the primary outcome (death or HF hospitalization) and secondary outcome (death, transplant, or LVAD) is plotted for both SSI groups using Kaplan–Meier curves. Between-group differences in freedom from event are tested using log-rank tests. Cox proportional hazards models were used to confirm the results of the log-rank test when adjusting for potential confounders. We determined potential confounding covariates and made adjustments with the influence of these explanatory variables held constant over time. The appropriateness of the proportional hazards assumption was verified by testing the interactions between each predictor and survival time; if the resulting time-dependent covariate is significant, then the proportional hazards assumption is violated for that predictor. A P value of <0.05 was considered significant.

Results

Simulated Strain Signature of an Electromechanical Substrate

The pattern of LV contraction heterogeneity because of an electromechanical LBBB-like substrate responsive to CRT was characterized by (1) early septal contraction associated with SPS_{POST} before AVO and (2) late posterolateral contraction associated with SRS_{SEPT} occurring at or after AVO (Figure 1A). The amplitude of LV contraction heterogeneity, and hence SPS_{POST}, SRS_{SEPT}, and SSI, increased linearly with the LBBB activation delay imposed. The simulated electromechanical LBBB substrate caused peak-to-peak radial strain delay, increasing from 96 ms in the synchronous failing heart to values >300 ms in all 3 LBBB simulations.

Simulated Strain Signatures of Non–Electrical Substrates

We observed that simulations of both posterolateral hypocontractility (Figure 1B) and scar (Figure 1C) in the synchronous failing heart showed that early systolic divergence of strain curves can occur in the absence of electrical activation delays. The relatively strong septal myocardium started thickening, causing thinning of the weakened posterolateral myocardium during the isovolumic contraction phase. This early systolic strain divergence did not reverse during ejection, unlike in the simulations of a pure electromechanical LBBB substrate (Figure 1A). The septal segments continued to thicken until the end of the ejection phase, whereas the weakened posterolateral segments stopped thinning once ejection began and remained stretched during most of the ejection phase. Both non–electrical substrates were associated with qualitatively

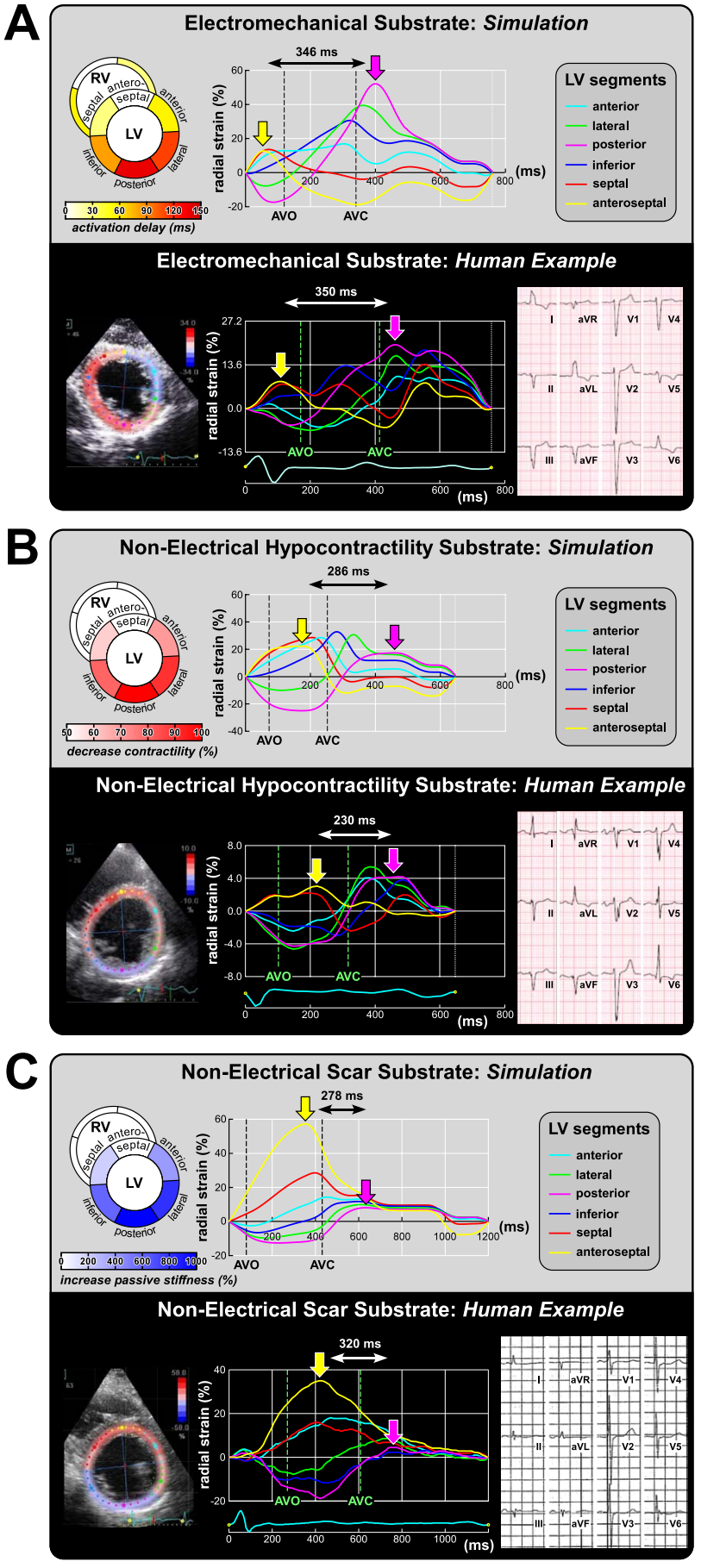

Figure 3. A, Electromechanical substrate: simulated vs measured mechanical discoordination. **Top**, Computer simulation of a left bundle branch block (LBBB)–like activation pattern with maximum posterior activation delay of 100 ms. Strain curves demonstrated a peak-to-peak radial strain delay of 346 ms. **Bottom**, Echocardiogram (**left**) from a 60-year-old heart failure (HF) patient with nonischemic cardiomyopathy (left ventricular [LV] ejection fraction, 23%). Before cardiac resynchronization therapy (CRT), QRS duration was 132 ms, with LBBB-type conduction delay on the ECG (**right**). Strain curves from mid LV level demonstrated a peak-to-peak radial strain delay of 350 ms (arrows) and SSI of 29%. This patient had improved LV ejection fraction (46%) and HF symptoms after CRT. **B**, Non–electrical hypocontractility substrate: simulated vs measured mechanical discoordination. **Top**, Computer simulation of a hypocontractility substrate with comparatively greater contractility decrease in posterolateral segments, combined with a LBBB-like activation pattern with maximum posterior activation delay of 50 ms. Strain curves demonstrated a peak-to-peak radial strain delay of 286 ms. **Bottom**, Echocardiogram (**left**) from a 65-year-old HF patient with nonischemic cardiomyopathy (LV ejection fraction, 27%). Before CRT, QRS duration was 130 ms, with an intraventricular conduction delay (**right**). Strain curves from mid LV level demonstrated a significant peak-to-peak radial strain delay of 230 ms (arrows) but low SSI of 5%. After CRT, this patient had no improvement in LV ejection fraction or HF symptoms. **C**, Non–electrical scar substrate: simulated vs measured mechanical discoordination. **Top**, Computer simulation of a scar substrate with increased passive stiffness along with decreased contractility (as in **B**) in the posterolateral segments, combined with a LBBB-like activation pattern with maximum posterior activation delay of 50 ms. Strain curves demonstrated a peak-to-peak radial strain delay of 278 ms. **Bottom**, Echocardiogram (**left**) from a 58-year-old HF patient with ischemic cardiomyopathy and inferior–posterior transmural infarction (LV ejection fraction, 25%). Before CRT, QRS duration was 130 ms, with an intraventricular conduction delay (**right**). Strain curves from mid LV level demonstrated a significant peak-to-peak radial strain delay of 320 ms (arrows) but low SSI of 4%. After CRT, this patient had no improvement in LV ejection fraction or HF symptoms. AVC indicates aortic valve closure; AVO, aortic valve opening; and RV, right ventricular.

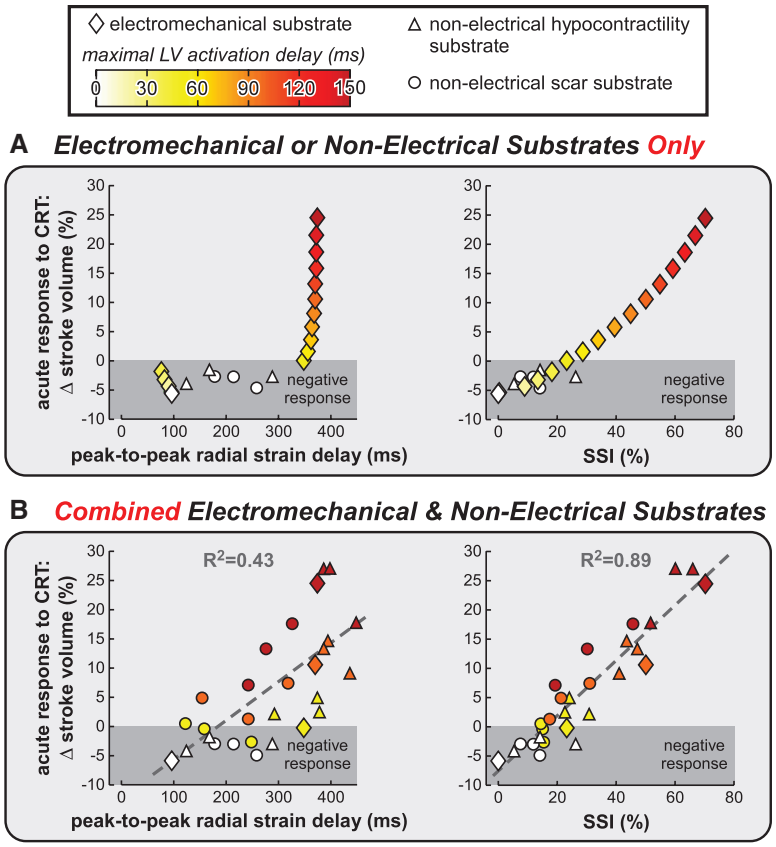

Figure 4. Simulated response to cardiac resynchronization therapy (CRT). **A**, Acute hemodynamic response to CRT as function of peak-to-peak radial strain delay (**left**) and systolic stretch index (SSI; **right**) for the simulations of pure electromechanical (simulated with 10-ms increments of color-coded maximal left ventricular [LV] activation delay) and pure non–electrical substrates only. **B**, Response to CRT as function of peak-to-peak radial strain delay (**left**) and SSI (**right**) for the simulations of 4 degrees of electromechanical LBBB substrate (color-coded) combined with 3 degrees of non–electrical hypocontractility (triangles) or scar (circles) substrates.

similar changes of LV radial strain curves, although pre-ejection thinning and postsystolic thickening of the posterolateral myocardium were larger in the compliant hypocontractile tissue (Figure 1B) than in the stiffer scarred tissue (Figure 1C).

Comparative Simulation and Patient Strain Data

Examples of the 3 different myocardial substrate simulations and comparable echocardiographic strain curves from HF patients (LVEF ≤35%) with their corresponding ECG are shown in Figure 3A–3C. Simulated and measured strain patterns showed good agreement, whereas no patient-specific fitting of model parameters except heart rate was performed. All 3 patient examples showed peak-to-peak radial strain delay >130 ms, that is, the cutoff value previously used to predict CRT response.[18] Figure 3A shows a patient with minimal QRS widening (132 ms) and strain patterns similar to the simulation of a pure electromechanical LBBB substrate. This patient had a peak-to-peak radial strain delay of 350 ms and a SSI of 29%. The patients in Figure 3B and 3C presented with similar QRS duration (130 ms) and baseline strain patterns resembling hypocontractility and scar substrate simulations, respectively. They had large peak-to-peak radial strain delays (230 and 320 ms, respectively) but low SSIs (5% and 4%, respectively).

Table 2. Baseline Characteristics of the Subgroup of Patients With Intermediate Electrocardiographic Criteria Grouped by Baseline SSI

Variables	Total Subgroup, n=113	SSI≥9.7%, n=51	SSI<9.7%, n=62	*P* Value
Age, y	67±11	66±10	67±11	0.56
Sex, male	89 (79%)	37 (73%)	52 (84%)	0.17
Ischemic disease, n	76 (67%)	31 (61%)	45 (73%)	0.23
Diabetes mellitus, n	39 (35%)	14 (28%)	25 (40%)	0.17
NYHA II/III, n	84 (80%)	38 (80%)	46 (80%)	1.00
LBBB 120–149 ms, n	38 (34%)	19 (37%)	19 (31%)	0.55
QRS duration, ms	149±26	153±29	145±24	0.08
β-blocker, n	97 (87%)	46 (90%)	51 (84%)	0.41
ACE/ARB inhibitor, n	95 (85%)	43 (84%)	52 (85%)	1.00
LVEF	23.8±6.0	24±5.5	23.5±6.4	0.63

ACE indicates angiotensin-converting enzyme; ARB, angiotensin II receptor blocker; LBBB, left bundle branch block; LVEF, left ventricular ejection fraction; NYHA, New York Heart Association; and SSI, systolic stretch index.

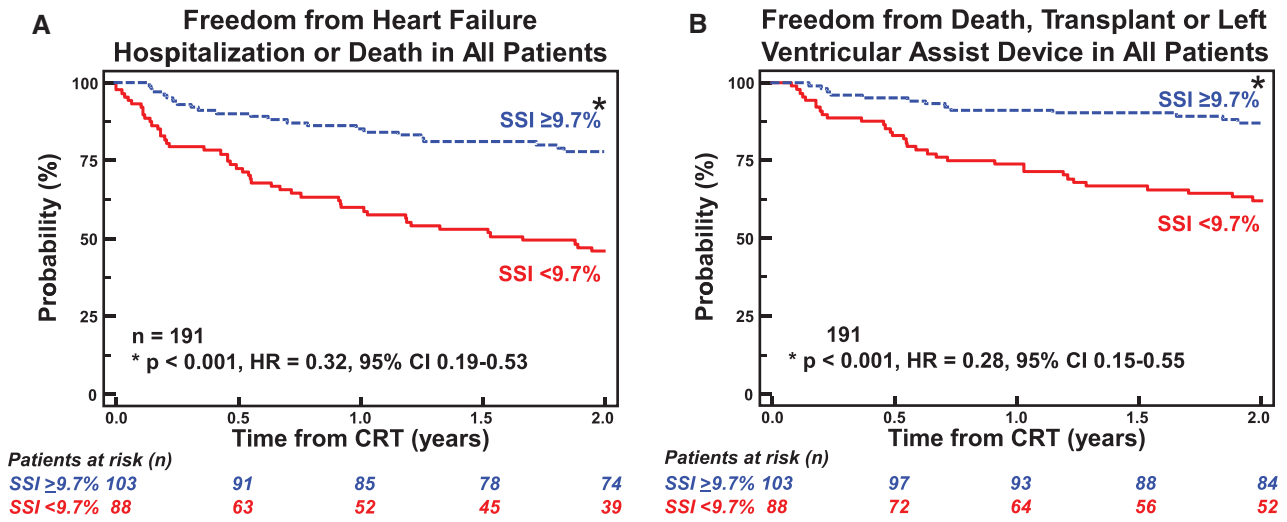

Figure 5. Clinical outcome in all patients. Kaplan–Meier curves showing probability of (**A**) freedom from heart failure hospitalization or death and (**B**) freedom from death, transplant, or left ventricular assist device after cardiac resynchronization therapy (CRT). *Baseline systolic stretch index (SSI) ≥9.7% was associated with a significantly more favorable clinical outcome. CI indicates confidence interval; and HR, hazard ratio.

Only the patient in Figure 3A responded favorably to CRT with clinical improvement in HF symptoms and LVEF.

SSI and Acute Hemodynamic Response to CRT

Simulations showed that a mild degree of electromechanical LBBB substrate (≥60 ms delay of posterolateral activation) was required for CRT to be hemodynamically beneficial (Figure 4A). Furthermore, there was no favorable acute CRT response and SSI was relatively small for all purely non–electrical substrate simulations, despite peak-to-peak radial strain delay of up to 288 ms. The same relations between acute CRT response and mechanical discoordination indices were observed for the simulations combining the electromechanical LBBB substrate with non–electrical substrates (Figure 4B). Both peak-to-peak radial strain delay and SSI correlated with acute changes in LV stroke volume after CRT, however, SSI correlated more closely with acute CRT response than peak-to-peak radial strain delay (R^2=0.89 versus 0.43).

Baseline SSI Analysis in Patients

Receiver operator characteristic analysis showed a baseline SSI of ≥9.7% to be most representative of CRT response. Table 1 shows baseline clinical characteristics of all patients together and grouped by SSI above and below this cutoff value. Patients with non-LBBB morphology mostly had intraventricular conduction delay (33%) and few had right bundle branch block (7%). Patients with SSI<9.7% tended to be older (68±11 versus 64±11 years; P=0.04), were more likely to be men (84% versus 65%; P=0.003), and were more likely to have ischemic disease (72% versus 51%;

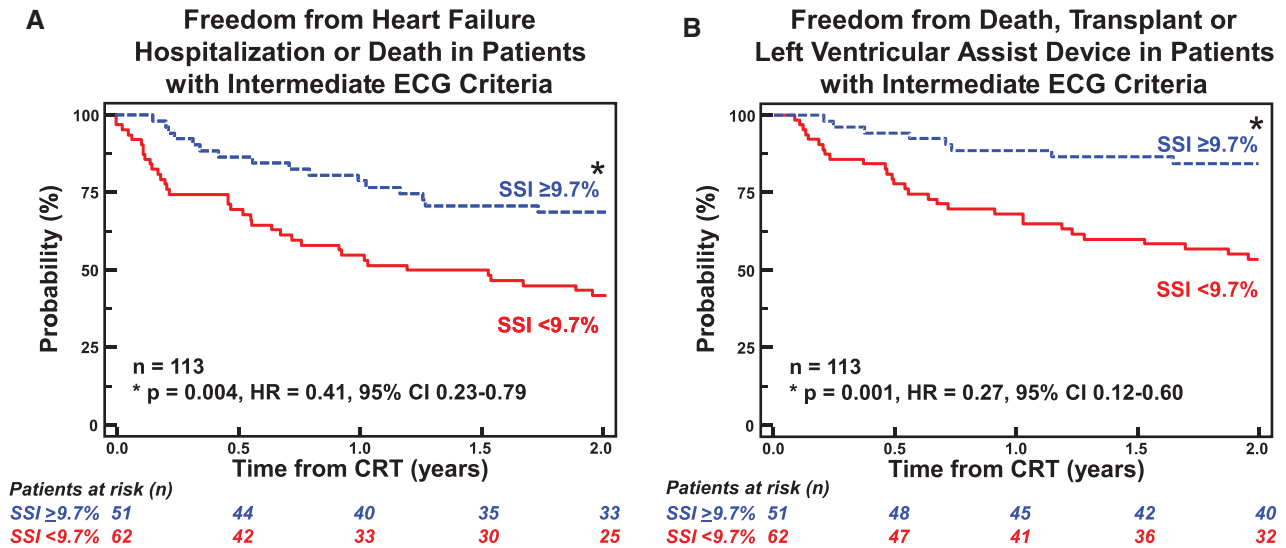

Figure 6. Clinical outcome in patients with intermediate electrocardiographic criteria. Kaplan–Meier curves showing probability of (**A**) freedom from heart failure hospitalization or death and (**B**) freedom from death, transplant, or left ventricular assist device after cardiac resynchronization therapy (CRT). *Baseline systolic stretch index (SSI) ≥9.7% was associated with a significantly more favorable clinical outcome. CI indicates confidence interval; and HR, hazard ratio.

P=0.003). Increased SSI was associated with LBBB electrocardiographic morphology and increased QRS duration as expected. Baseline clinical characteristics of patients with intermediate electrocardiographic criteria showed no confounding associations with SSI (Table 2), except QRS duration as a potential covariate (*P*=0.08).

Long-Term Clinical Outcomes: All Patients

For the full cohort of 191 patients over a 2-year interval, the combined end point of HF hospitalization or death was met in 69 patients (51 by first HF hospitalization end point and 18 by deaths). SSI≥9.7% was associated with less HF hospitalizations or deaths (hazard ratio, 0.32; 95% confidence interval, 0.19–0.53; *P*<0.001; Figure 5A). The combined end point of death, heart transplant, or LVAD was met in 46 patients (33 deaths, 5 transplants, and 8 LVADs). SSI≥9.7% was also associated with a more favorable outcome with respect to this combined end point of hard events (hazard ratio, 0.28; 95% confidence interval, 0.15–0.55; *P*<0.001; Figure 5B). SSI≥9.7% remained independently associated with both combined end points (*P*<0.05) after adjustments for the potential covariates of age, sex, and ischemic disease.

Long-Term Clinical Outcomes: Intermediate Electrocardiographic Criteria Subgroup

Among the subgroup of 113 patients with intermediate electrocardiographic criteria, SSI≥9.7% was associated with a more favorable clinical outcome with respect to HF hospitalization or death (hazard ratio, 0.41; 95% confidence interval, 0.23–0.79; *P*=0.004, Figure 6A) and more favorable outcomes with respect to death, transplant, or LVAD (hazard ratio, 0.27; 95% confidence interval, 0.12–0.60; *P*=0.001; Figure 6B). In this subgroup, SSI≥9.7% remained independently associated with both combined end points (*P*<0.05) after adjustment for the potential covariate of QRS duration. The potential confounding variables of age, sex, ischemic disease, QRS duration, and morphology known to be associated with CRT response were tested in univariable and multivariable analysis (Table 3). Only QRS duration and LBBB morphology were significantly associated with event-free survival in multivariable analysis when SSI was taken into account.

Comparison of Baseline Discoordination Indices

For all patients, SSI, peak-to-peak radial strain delay, and IVMD were significantly associated with both combined end

Table 3. Univariable and Multivariable Analysis of Associations With Clinical Outcomes

	Univariable		Multivariable	
	HR (95% CI)	*P* Value	HR (95% CI)	*P* Value
All patients, n=191				
Outcome: Heart failure hospitalization or death				
Sex, female	0.56 (0.30–1.04)	0.06	…	…
Ischemic disease	1.84 (1.09–3.09)	0.02	…	…
QRS duration, 10 ms increase	0.83 (0.75–0.92)	<0.001	0.88 (0.79–0.97)	0.008
LBBB morphology	0.46 (0.20–0.74)	0.001	0.61 (0.37–1.00)	0.05
SSI≥9.7%	0.32 (0.19–0.53)	<0.001	0.34 (0.20–0.59)	<0.001
Outcome: Death, transplant, or LVAD therapy				
Sex, female	0.56 (0.26–1.20)	0.14	…	…
Ischemic disease	1.43 (0.77–2.66)	0.25	…	…
QRS duration (10 ms increase)	0.80 (0.70–0.91)	0.001	0.86 (0.76–0.98)	0.02
LBBB morphology	0.31 (0.17–0.56)	<0.001	0.40 (0.22–0.75)	0.004
SSI≥9.7%	0.28 (0.15–0.55)	<0.001	0.31 (0.16–0.63)	0.001
Intermediate electrocardiographic criteria patients, n=113				
Outcome: Heart failure hospitalization or death				
Sex, female	0.52 (0.23–1.14)	0.10	…	…
Ischemic disease	1.85 (0.97–3.54)	0.06	…	…
QRS duration, 10 ms increase	0.88 (0.79–0.99)	0.03	0.88 (0.79–0.97)	0.04
LBBB morphology	0.65 (0.35–1.21)	0.17	…	…
SSI≥9.7%	0.41 (0.23–0.79)	0.004	0.41 (0.22–0.68)	0.005
Outcome: Death, transplant, or LVAD therapy				
Sex, female	0.54 (0.21–1.37)	0.19	…	…
Ischemic disease	1.36 (0.66–2.80)	0.41	…	…
QRS duration, 10 ms increase	0.86 (0.74–1.00)	0.05	0.86 (0.74–1.00)	0.05
LBBB morphology	0.41 (0.18–0.93)	0.03	0.37 (0.16–0.84)	0.02
SSI≥9.7%	0.27 (0.12–0.60)	0.001	0.27 (0.12–0.63)	0.002

CI indicates confidence interval; HR, hazard ratio; LBBB, left bundle branch block; LVAD, left ventricular assist device; and SSI, systolic stretch index.

points (Table 4). SSI was most closely associated with both combined end points, followed by IVMD and peak-to-peak radial strain delay, respectively. In the intermediate electrocardiographic criteria subgroup, SSI and its component SRS_{SEPT} were associated with both combined end points, whereas peak-to-peak radial strain delay was only associated with the combined end point of death, transplant, or LVAD, and IVMD was not associated with either combined end point. SSI outperformed both SPS_{POST} and SRS_{SEPT} in its association with the combined end point of death, transplant, or LVAD in all patients and the intermediate electrocardiographic criteria subgroup.

Discussion

We used computer simulations to differentiate patterns of LV mechanical discoordination arising from electromechanical substrates that are responsive to CRT from discoordination patterns caused by non–electrical substrates unresponsive to CRT. Specifically, SPS_{POST} and SRS_{SEPT}, unified by the newly developed SSI, indicated the myocardial deformation signature of the electromechanical substrate associated with CRT response. Computer simulations enabled manipulation of regional electrical activation delay, contractility, and passive stiffness that cannot be controlled independently in animal models or humans. Simulations also demonstrated that peak-to-peak strain measures of dyssynchrony could ambiguously represent electromechanical and non–electrical substrates, which may explain the failure of these measures to predict response in patients with narrow QRS.[5,6]

Prospective application of echocardiographic SSI analysis to a consecutive series of CRT recipients showed that a baseline SSI≥9.7% was associated with a more favorable response to CRT with respect to the clinical outcomes of the primary end point of HF hospitalizations or death and also the secondary combined end point of death, transplant, or LVAD. Unlike other indices of mechanical dyssynchrony, SSI was independently associated with more favorable clinical outcomes after CRT in patients with intermediate electrocardiographic criteria of QRS duration of 120 to 149 ms or non-LBBB morphology. Furthermore, SSI was a better predictor of CRT response compared with peak-to-peak radial strain delay or IVMD and better than QRS duration or morphology alone. The combination of our computational and clinical findings extends the understanding of confounding causes of LV mechanical discoordination in HF patients with low LVEF.

Complexity of LV Mechanical Discoordination

Our model simulations showed how 3 candidate discoordination substrates likely to exist in patients with HF can explain the complexity and diversity of regional LV myocardial strain patterns as measured in CRT candidates. Experimental studies in a canine model of LBBB[19–21] have led to a characterization of the pattern of LV mechanical discoordination caused by LBBB as early systolic septal contraction and posterolateral wall stretch followed by SRS_{SEPT} and delayed posterolateral contraction, respectively. These mechanical consequences of LBBB were consistently found to be associated with impaired cardiac pump function in experimental and computational models of LBBB.[14,19–22] Furthermore, it has been shown that a critical degree of such an electromechanical substrate must be present for CRT to be beneficial.[7,23]

The characteristic LBBB pattern of LV contraction heterogeneity described above is not consistently observed in CRT patient cohorts.[24] Our simulations suggest that this dissociation between QRS widening and LV contraction heterogeneity can be explained by the coexistence of non–electrical substrates, such as regional hypocontractility or scar. Although non–electrical substrates changed the overall pattern of LV contraction heterogeneity when simulated in combination with an electromechanical LBBB substrate, radial strain features, such as SPS_{POST} and SRS_{SEPT}, arising from the electromechanical substrate were still present, albeit to a lesser extent. Myocardial scar or hypocontractility did not preclude positive hemodynamic CRT response in either our simulations or

Table 4. Associations of Dyssynchrony and Discoordination Indices With Clinical Outcomes

	HF Hospitalizations or Death		Death, Transplant, or LVAD Therapy	
	HR (95% CI)	*P* Value	HR (95% CI)	*P* Value
All patients, n=191				
Peak-to-peak strain delay ≥130 ms	0.56 (0.34–0.91)	0.018	0.49 (0.27–0.88)	0.017
IVMD≥40 ms	0.40 (0.24–0.66)	<0.001	0.39 (0.21–0.72)	0.003
SPS_{POST}≥2.3%	0.41 (0.25–0.68)	<0.001	0.58 (0.32–1.06)	0.080
SRS_{SEPT}≥5.8%	0.33 (0.21–0.54)	<0.001	0.35 (0.19–0.64)	0.001
SSI≥9.7%	0.32 (0.19–0.53)	<0.001	0.28 (0.15–0.55)	<0.001
Intermediate electrocardiographic criteria patients, n=113				
Peak-to-peak strain delay ≥130 ms	0.59 (0.34–1.03)	0.063	0.50 (0.26–0.95)	0.033
IVMD≥40 ms	0.64 (0.35–1.17)	0.149	0.63 (0.30–1.31)	0.216
SPS_{POST}≥2.3%	0.49 (0.27–0.88)	0.017	0.62 (0.31–1.23)	0.168
SRS_{SEPT}≥5.8%	0.42 (0.24–0.75)	0.003	0.38 (0.20–0.77)	0.007
SSI≥9.7%	0.41 (0.23–0.79)	0.004	0.27 (0.12–0.60)	0.001

CI indicates confidence interval; HF, heart failure; HR, hazard ratio; IVMD, interventricular mechanical delay; LVAD, left ventricular assist device; SPS_{POST}, posterolateral systolic prestretch; SRS_{SEPT}, septal systolic rebound stretch; and SSI, systolic stretch index.

animal models of HF with LBBB and myocardial infarction.[25] Moreover, subsets of wide QRS patients with non-LBBB or even right bundle branch block morphologies have been shown to respond to CRT provided that contralateral systolic stretch as described above is present.[24]

Peak-to-Peak Dyssynchrony Measures Are Not Specific to Electrical Substrates

Mechanical dyssynchrony, in terms of time-to-peak strain or velocity measurements, has been reported to commonly occur in HF patients with narrow QRS complex (<130 ms).[5,26–28] The negative outcome of the Echocardiography Guided Cardiac Resynchronization Therapy (EchoCRT) trial,[6] however, suggests that time-to-peak dyssynchrony does not necessarily represent an electromechanical substrate treatable with CRT. Our simulations support this hypothesis by showing that a peak-to-peak radial strain delay ≥130 ms (the cutoff used for EchoCRT patient inclusion) can occur in synchronously activated failing hearts with non–electrical substrates of mechanical discoordination.

SSI Identifies Electrical Substrates Responsive to CRT

These findings support a mechanistic approach for quantifying mechanical discoordination, instead of dyssynchrony, integrating timing and amplitude of strain features specific to the electromechanical substrate responsive to CRT.[29–31] To that end, SSI was designed to capture 2 key radial strain features of the electromechanical substrate responsive to CRT. First, SPS_{POST} reveals an activation delay of the lateral wall tissue, which is stretched by early-activated septal tissue. Second, SRS_{SEPT} detects the mechanical effect of the forcefully contracting late-activated tissue on early-activated septal tissue. Longitudinal strain–based SRS_{SEPT} has previously been shown to be a predictor of clinical outcome after CRT in HF patients with LBBB morphology.[23] By combining SPS_{POST} and SRS_{SEPT}, the SSI is intended as an easily implemented form of pattern recognition that detects a septal-to-posterolateral electrical activation delay. In our simulations, this electromechanical substrate represented by SSI related linearly to acute hemodynamic response to CRT. In the presence of regional hypocontractility or scar, both SSI and acute CRT response were lower, while maintaining their linear relation. Hence, simulations supported SSI to be a predictor of acute CRT response in a wide range of pathophysiological circumstances.

Although clear associations of QRS duration and QRS morphology with CRT response have been shown in clinical trials, the widest variability in CRT response was observed among patients with QRS duration of 120 to 149 ms or non-LBBB.[32,33] Accordingly, the greatest opportunity to improve patient selection is in this intermediate electrocardiographic criteria group. When comparing IVMD as a simple and reproducible parameter associated with response to CRT in patients with wide QRS and LBBB morphology,[14,34] SSI performed comparatively better. In addition, baseline SSI was more closely associated with CRT response than IVMD in the cohort with intermediate electrocardiographic criteria (QRS duration of 120 to 149 ms or non-LBBB morphology). Accordingly, the more time-consuming strain analysis seems to be of particular value over the simpler IVMD in these patients in the intermediate electrocardiographic group.

Study Limitations

Our simulations may not include all pathophysiological variables encountered in patients. Heterogeneities in conduction velocity related to non–electrical substrates[35] were not included. Simulations only allowed evaluation of acute hemodynamic response to CRT. Furthermore, ventricular geometry in CircAdapt is highly simplified, which may have caused the systematic overestimation of simulated radial strain values and thus SSI.

Although SSI was prospectively applied in a blinded fashion to an existing data set, it is an acknowledged limitation that patients were not prospectively enrolled with SSI performed before CRT implantation. This study was limited to sinus rhythm to reflect the patient population studied and the current CRT clinical guidelines.[1] Application to patients in atrial fibrillation may be of interest for future study. High-quality speckle-tracking echocardiography may only be applied to technically adequate images. It is a known limitation that technically adequate image quality is required for speckle-tracking strain analysis, and our exclusion rate of 9% is similar to previous studies.[2,6,18] Continued technological improvements in image acquisition and refinements in analysis may likely reduce this exclusion rate in the future. The user interface for locating the echocardiographic regions of interest to generate the radial strain curves requires training and experience, although SSI analysis itself was computer-automated and objective. Semiautomated image analysis has promise for reducing this potential source of variability. Other variables affecting CRT response, such as scar burden,[36] LV lead position,[37] or atrioventricular–ventriculoventricular delay optimization,[38] were not part of this study.

Conclusions

Computer simulations were used to differentiate patterns of LV mechanical discoordination caused by electromechanical substrates that are responsive to CRT from those caused by non–electrical substrates unresponsive to CRT. The combination of SPS_{POST} and SRS_{SEPT}, unified by the SSI, specifically represented an electromechanical substrate responsive to CRT. Baseline SSI identified patients who benefited more favorably from CRT, including those with intermediate electrocardiographic criteria, where CRT response is less certain by ECG alone.

Acknowledgments

We are grateful to Dr Michael Gold (Medical University of South Carolina, Charleston, South Carolina) for his thoughtful review of the article and valuable suggestions.

Sources of Funding

Dr Lumens received a grant within the framework of the Dr E. Dekker program of the Dutch Heart Foundation (NHS-2012T010). Dr Gorcsan received research grant support from Biotronik, GE, Medtronic, St. Jude Medical, and Toshiba. Dr Prinzen received

research grants from Medtronic, Boston Scientific, EBR Systems, Biological Delivery Systems (Johnson & Johnson), MSD, and Proteus Biomedical. Dr Schwartzman received research grants from Medtronic, Boston Scientific, and Biosense.

Disclosures

Dr Prinzen is advisor to St. Jude Medical. Dr Schwartzman is consultant for Boston Scientific, Atricure, Avery Dennison, Biosense, Quant MD, and Epicardial Frontiers. The other authors report no conflicts.

References

1. Tracy CM, Epstein AE, Darbar D, DiMarco JP, Dunbar SB, Estes NA 3rd, Ferguson TB Jr, Hammill SC, Karasik PE, Link MS, Marine JE, Schoenfeld MH, Shanker AJ, Silka MJ, Stevenson LW, Stevenson WG, Varosy PD, Ellenbogen KA, Freedman RA, Gettes LS, Gillinov AM, Gregoratos G, Hayes DL, Page RL, Stevenson LW, Sweeney MO; American College of Cardiology Foundation; American Heart Association Task Force on Practice Guidelines; Heart Rhythm Society. 2012 ACCF/AHA/HRS focused update of the 2008 guidelines for device-based therapy of cardiac rhythm abnormalities: a report of the American College of Cardiology Foundation/American Heart Association Task Force on Practice Guidelines and the Heart Rhythm Society. [corrected]. *Circulation*. 2012;126:1784–1800. doi: 10.1161/CIR.0b013e3182618569.
2. Gorcsan J 3rd, Oyenuga O, Habib PJ, Tanaka H, Adelstein EC, Hara H, McNamara DM, Saba S. Relationship of echocardiographic dyssynchrony to long-term survival after cardiac resynchronization therapy. *Circulation*. 2010;122:1910–1918. doi: 10.1161/CIRCULATIONAHA.110.954768.
3. Kass DA. An epidemic of dyssynchrony: but what does it mean? *J Am Coll Cardiol*. 2008;51:12–17. doi: 10.1016/j.jacc.2007.09.027.
4. Chung ES, Leon AR, Tavazzi L, Sun JP, Nihoyannopoulos P, Merlino J, Abraham WT, Ghio S, Leclercq C, Bax JJ, Yu CM, Gorcsan J 3rd, St John Sutton M, De Sutter J, Murillo J. Results of the Predictors of Response to CRT (PROSPECT) trial. *Circulation*. 2008;117:2608–2616. doi: 10.1161/CIRCULATIONAHA.107.743120.
5. Beshai JF, Grimm RA, Nagueh SF, Baker JH 2nd, Beau SL, Greenberg SM, Pires LA, Tchou PJ; RethinQ Study Investigators. Cardiac-resynchronization therapy in heart failure with narrow QRS complexes. *N Engl J Med*. 2007;357:2461–2471. doi: 10.1056/NEJMoa0706695.
6. Ruschitzka F, Abraham WT, Singh JP, Bax JJ, Borer JS, Brugada J, Dickstein K, Ford I, Gorcsan J 3rd, Gras D, Krum H, Sogaard P, Holzmeister J; EchoCRT Study Group. Cardiac-resynchronization therapy in heart failure with a narrow QRS complex. *N Engl J Med*. 2013;369:1395–1405. doi: 10.1056/NEJMoa1306687.
7. Zareba W, Klein H, Cygankiewicz I, Hall WJ, McNitt S, Brown M, Cannom D, Daubert JP, Eldar M, Gold MR, Goldberger JJ, Goldenberg I, Lichstein E, Pitschner H, Rashtian M, Solomon S, Viskin S, Wang P, Moss AJ; MADIT-CRT Investigators. Effectiveness of cardiac resynchronization therapy by QRS morphology in the Multicenter Automatic Defibrillator Implantation Trial-Cardiac Resynchronization Therapy (MADIT-CRT). *Circulation*. 2011;123:1061–1072. doi: 10.1161/CIRCULATIONAHA.110.960898.
8. Bristow MR, Saxon LA, Boehmer J, Krueger S, Kass DA, De Marco T, Carson P, DiCarlo L, DeMets D, White BG, DeVries DW, Feldman AM; Comparison of Medical Therapy, Pacing, and Defibrillation in Heart Failure (COMPANION) Investigators. Cardiac-resynchronization therapy with or without an implantable defibrillator in advanced chronic heart failure. *N Engl J Med*. 2004;350:2140–2150. doi: 10.1056/NEJMoa032423.
9. Abraham WT, Fisher WG, Smith AL, Delurgio DB, Leon AR, Loh E, Kocovic DZ, Packer M, Clavell AL, Hayes DL, Ellestad M, Trupp RJ, Underwood J, Pickering F, Truex C, McAtee P, Messenger J; MIRACLE Study Group. Multicenter InSync Randomized Clinical Evaluation. Cardiac resynchronization in chronic heart failure. *N Engl J Med*. 2002;346:1845–1853. doi: 10.1056/NEJMoa013168.
10. Cleland JG, Daubert JC, Erdmann E, Freemantle N, Gras D, Kappenberger L, Tavazzi L; Cardiac Resynchronization-Heart Failure (CARE-HF) Study Investigators. The effect of cardiac resynchronization on morbidity and mortality in heart failure. *N Engl J Med*. 2005;352:1539–1549. doi: 10.1056/NEJMoa050496.
11. Lumens J, Delhaas T, Kirn B, Arts T. Three-wall segment (TriSeg) model describing mechanics and hemodynamics of ventricular interaction. *Ann Biomed Eng*. 2009;37:2234–2255. doi: 10.1007/s10439-009-9774-2.
12. Walmsley J, Arts T, Derval N, Bordachar P, Cochet H, Ploux S, Prinzen FW, Delhaas T, Lumens J. Fast simulation of mechanical heterogeneity in the electrically asynchronous heart using the MultiPatch module. *PLoS Comput Biol*. 2015;11:e1004284. doi: 10.1371/journal.pcbi.1004284.
13. Leenders GE, Lumens J, Cramer MJ, De Boeck BW, Doevendans PA, Delhaas T, Prinzen FW. Septal deformation patterns delineate mechanical dyssynchrony and regional differences in contractility: analysis of patient data using a computer model. *Circ Heart Fail*. 2012;5:87–96. doi: 10.1161/CIRCHEARTFAILURE.111.962704.
14. Lumens J, Leenders GE, Cramer MJ, De Boeck BW, Doevendans PA, Prinzen FW, Delhaas T. Mechanistic evaluation of echocardiographic dyssynchrony indices: patient data combined with multiscale computer simulations. *Circ Cardiovasc Imaging*. 2012;5:491–499. doi: 10.1161/CIRCIMAGING.112.973446.
15. Lumens J, Ploux S, Strik M, Gorcsan J 3rd, Cochet H, Derval N, Strom M, Ramanathan C, Ritter P, Haïssaguerre M, Jaïs P, Arts T, Delhaas T, Prinzen FW, Bordachar P. Comparative electromechanical and hemodynamic effects of left ventricular and biventricular pacing in dyssynchronous heart failure: electrical resynchronization versus left-right ventricular interaction. *J Am Coll Cardiol*. 2013;62:2395–2403. doi: 10.1016/j.jacc.2013.08.715.
16. Walker JC, Ratcliffe MB, Zhang P, Wallace AW, Fata B, Hsu EW, Saloner D, Guccione JM. MRI-based finite-element analysis of left ventricular aneurysm. *Am J Physiol Heart Circ Physiol*. 2005;289:H692–H700. doi: 10.1152/ajpheart.01226.2004.
17. De Boeck BW, Teske AJ, Meine M, Leenders GE, Cramer MJ, Prinzen FW, Doevendans PA. Septal rebound stretch reflects the functional substrate to cardiac resynchronization therapy and predicts volumetric and neurohormonal response. *Eur J Heart Fail*. 2009;11:863–871. doi: 10.1093/eurjhf/hfp107.
18. Suffoletto MS, Dohi K, Cannesson M, Saba S, Gorcsan J 3rd. Novel speckle-tracking radial strain from routine black-and-white echocardiographic images to quantify dyssynchrony and predict response to cardiac resynchronization therapy. *Circulation*. 2006;113:960–968. doi: 10.1161/CIRCULATIONAHA.105.571455.
19. Gjesdal O, Remme EW, Opdahl A, Skulstad H, Russell K, Kongsgaard E, Edvardsen T, Smiseth OA. Mechanisms of abnormal systolic motion of the interventricular septum during left bundle-branch block. *Circ Cardiovasc Imaging*. 2011;4:264–273. doi: 10.1161/CIRCIMAGING.110.961417.
20. Helm RH, Leclercq C, Faris OP, Ozturk C, McVeigh E, Lardo AC, Kass DA. Cardiac dyssynchrony analysis using circumferential versus longitudinal strain: implications for assessing cardiac resynchronization. *Circulation*. 2005;111:2760–2767. doi: 10.1161/CIRCULATIONAHA.104.508457.
21. Vernooy K, Verbeek XA, Peschar M, Crijns HJ, Arts T, Cornelussen RN, Prinzen FW. Left bundle branch block induces ventricular remodelling and functional septal hypoperfusion. *Eur Heart J*. 2005;26:91–98. doi: 10.1093/eurheartj/ehi008.
22. Kerckhoffs RC, Omens JH, McCulloch AD, Mulligan LJ. Ventricular dilation and electrical dyssynchrony synergistically increase regional mechanical nonuniformity but not mechanical dyssynchrony: a computational model. *Circ Heart Fail*. 2010;3:528–536. doi: 10.1161/CIRCHEARTFAILURE.109.862144.
23. Leenders GE, De Boeck BW, Teske AJ, Meine M, Bogaard MD, Prinzen FW, Doevendans PA, Cramer MJ. Septal rebound stretch is a strong predictor of outcome after cardiac resynchronization therapy. *J Card Fail*. 2012;18:404–412. doi: 10.1016/j.cardfail.2012.02.001.
24. Hara H, Oyenuga OA, Tanaka H, Adelstein EC, Onishi T, McNamara DM, Schwartzman D, Saba S, Gorcsan J 3rd. The relationship of QRS morphology and mechanical dyssynchrony to long-term outcome following cardiac resynchronization therapy. *Eur Heart J*. 2012;33:2680–2691. doi: 10.1093/eurheartj/ehs013.
25. Rademakers LM, van Kerckhoven R, van Deursen CJ, Strik M, van Hunnik A, Kuiper M, Lampert A, Klersy C, Leyva F, Auricchio A, Maessen JG, Prinzen FW. Myocardial infarction does not preclude electrical and hemodynamic benefits of cardiac resynchronization therapy in dyssynchronous canine hearts. *Circ Arrhythm Electrophysiol*. 2010;3:361–368. doi: 10.1161/CIRCEP.109.931865.
26. Bleeker GB, Holman ER, Steendijk P, Boersma E, van der Wall EE, Schalij MJ, Bax JJ. Cardiac resynchronization therapy in patients with a narrow QRS complex. *J Am Coll Cardiol*. 2006;48:2243–2250. doi: 10.1016/j.jacc.2006.07.067.
27. Yu CM, Chan YS, Zhang Q, Yip GW, Chan CK, Kum LC, Wu L, Lee AP, Lam YY, Fung JW. Benefits of cardiac resynchronization therapy for heart failure patients with narrow QRS complexes and coexisting systolic

asynchrony by echocardiography. *J Am Coll Cardiol*. 2006;48:2251–2257. doi: 10.1016/j.jacc.2006.07.054.
28. Tanaka H, Tanabe M, Simon MA, Starling RC, Markham D, Thohan V, Mather P, McNamara DM, Gorcsan J 3rd. Left ventricular mechanical dyssynchrony in acute onset cardiomyopathy: association of its resolution with improvements in ventricular function. *JACC Cardiovasc Imaging*. 2011;4:445–456. doi: 10.1016/j.jcmg.2011.02.012.
29. Kydd AC, Khan FZ, O'Halloran D, Pugh PJ, Virdee MS, Dutka DP. Radial strain delay based on segmental timing and strain amplitude predicts left ventricular reverse remodeling and survival after cardiac resynchronization therapy. *Circ Cardiovasc Imaging*. 2013;6:177–184. doi: 10.1161/CIRCIMAGING.112.000191.
30. Lim P, Buakhamsri A, Popovic ZB, Greenberg NL, Patel D, Thomas JD, Grimm RA. Longitudinal strain delay index by speckle tracking imaging: a new marker of response to cardiac resynchronization therapy. *Circulation*. 2008;118:1130–1137. doi: 10.1161/CIRCULATIONAHA.107.750190.
31. Russell K, Opdahl A, Remme EW, Gjesdal O, Skulstad H, Kongsgaard E, Edvardsen T, Smiseth OA. Evaluation of left ventricular dyssynchrony by onset of active myocardial force generation: a novel method that differentiates between electrical and mechanical etiologies. *Circ Cardiovasc Imaging*. 2010;3:405–414. doi: 10.1161/CIRCIMAGING.109.905539.
32. Cleland JG, Abraham WT, Linde C, Gold MR, Young JB, Claude Daubert J, Sherfesee L, Wells GA, Tang AS. An individual patient meta-analysis of five randomized trials assessing the effects of cardiac resynchronization therapy on morbidity and mortality in patients with symptomatic heart failure. *Eur Heart J*. 2013;34:3547–3556. doi: 10.1093/eurheartj/eht290.
33. Gold MR, Thébault C, Linde C, Abraham WT, Gerritse B, Ghio S, St John Sutton M, Daubert JC. Effect of QRS duration and morphology on cardiac resynchronization therapy outcomes in mild heart failure: results from the Resynchronization Reverses Remodeling in Systolic Left Ventricular Dysfunction (REVERSE) study. *Circulation*. 2012;126:822–829. doi: 10.1161/CIRCULATIONAHA.112.097709.
34. Miyazaki C, Redfield MM, Powell BD, Lin GM, Herges RM, Hodge DO, Olson LJ, Hayes DL, Espinosa RE, Rea RF, Bruce CJ, Nelson SM, Miller FA, Oh JK. Dyssynchrony indices to predict response to cardiac resynchronization therapy: a comprehensive prospective single-center study. *Circ Heart Fail*. 2010;3:565–573. doi: 10.1161/CIRCHEARTFAILURE.108.848085.
35. Lambiase PD, Rinaldi A, Hauck J, Mobb M, Elliott D, Mohammad S, Gill JS, Bucknall CA. Non-contact left ventricular endocardial mapping in cardiac resynchronisation therapy. *Heart*. 2004;90:44–51.
36. Adelstein EC, Saba S. Scar burden by myocardial perfusion imaging predicts echocardiographic response to cardiac resynchronization therapy in ischemic cardiomyopathy. *Am Heart J*. 2007;153:105–112. doi: 10.1016/j.ahj.2006.10.015.
37. Saba S, Marek J, Schwartzman D, Jain S, Adelstein E, White P, Oyenuga OA, Onishi T, Soman P, Gorcsan J 3rd. Echocardiography-guided left ventricular lead placement for cardiac resynchronization therapy: results of the speckle tracking assisted resynchronization therapy for Electrode Region trial. *Circ Heart Fail*. 2013;6:427–434. doi: 10.1161/CIRCHEARTFAILURE.112.000078.
38. Whinnett ZI, Francis DP, Denis A, Willson K, Pascale P, van Geldorp I, De Guillebon M, Ploux S, Ellenbogen K, Haïssaguerre M, Ritter P, Bordachar P. Comparison of different invasive hemodynamic methods for AV delay optimization in patients with cardiac resynchronization therapy: implications for clinical trial design and clinical practice. *Int J Cardiol*. 2013;168:2228–2237. doi: 10.1016/j.ijcard.2013.01.216.

CLINICAL PERSPECTIVE

Left ventricular mechanical discoordination, often referred to as dyssynchrony, is often observed in patients with heart failure regardless of QRS duration. However, the role of dyssynchrony to improve patient selection for cardiac resynchronization therapy (CRT) has been confusing, and electrocardiographic criteria remain with QRS duration >150 ms and left bundle branch block most favored. We used computer simulations to differentiate patterns of left ventricular mechanical discoordination arising from electromechanical substrates responsive to CRT from patterns of discoordination caused by unresponsive non–electrical substrates, such as regional contractile heterogeneity or scar. Simulations demonstrated that peak-to-peak strain measures of dyssynchrony could ambiguously represent electromechanical and non–electrical substrates. Simulations also revealed that posterolateral systolic prestretch and septal systolic rebound stretch, combined as systolic stretch index, can identify the electromechanical substrate associated with CRT response. Application of echocardiographic systolic stretch index analysis to a series of CRT recipients showed that a baseline systolic stretch index ≥9.7% was associated with a more favorable response to CRT, in terms of decreased heart failure hospitalizations, death, transplants, or mechanical support. Systolic stretch index was independently associated with more favorable clinical outcomes after CRT in patients with intermediate electrocardiographic criteria of QRS duration of 120 to 149 ms or non–left bundle branch block morphology. This observation has promise clinically because selecting patients for CRT with intermediate QRS duration or non–left bundle branch block is less clear. Our synergistic computational and clinical findings support that a mechanistic approach to quantifying mechanical discoordination extends the understanding of confounding causes of left ventricular mechanical discoordination in patients with heart failure and has the potential to improve patient selection for CRT.